



Perturbation-free measurement of *in situ* di-nitrogen emissions from denitrification in nitrate-rich aquatic ecosystems



Shuping Qin^{a, b}, Timothy Clough^c, Jiafa Luo^d, Nicole Wrage-Mönnig^e, Oene Oenema^f, Yuming Zhang^a, Chunsheng Hu^{a, *}

^a Key Laboratory of Agricultural Water Resources, Center for Agricultural Resources Research, Institute of Genetic and Developmental Biology, The Chinese Academy of Sciences, 286 Huaizhong Road, Shijiazhuang, 050021, Hebei, China

^b Fujian Provincial Key Laboratory of Soil Environmental Health and Regulation, College of Resources and Environment, Fujian Agriculture and Forestry University, Fuzhou, 350002, China

^c Lincoln University, Department of Agriculture & Life Sciences, Lincoln, New Zealand

^d Land and Environment, AgResearch, Hamilton, 3240, New Zealand

^e University of Rostock, Department of Agriculture and The Environment, Grassland and Fodder Sciences, Rostock, Germany

^f Wageningen University and Research, Alterra, Wageningen, The Netherlands

ARTICLE INFO

Article history:

Received 28 June 2016

Received in revised form

20 October 2016

Accepted 10 November 2016

Available online 12 November 2016

Keywords:

Denitrification
Isotopic fractionation
Reactive nitrogen
Nitrogen loss
N₂O reduction

ABSTRACT

Increased production of reactive nitrogen (Nr) from atmospheric di-nitrogen (N₂) has greatly contributed to increased food production. However, enriching the biosphere with Nr has also caused a series of negative effects on global ecosystems, especially aquatic ecosystems. The main pathway converting Nr back into the atmospheric N₂ pool is the last step in the denitrification process. Despite several attempts, there is still a need for perturbation-free methods for measuring *in situ* N₂ fluxes from denitrification in aquatic ecosystems at the field scale. Such a method is needed to comprehensively quantify the N₂ fluxes from aquatic ecosystems. Here we observed linear relationships between the δ¹⁵N-N₂O signatures and the logarithmically transformed N₂O/(N₂+N₂O) emission ratios. Through independent measurements, we verified that the perturbation-free N₂ flux from denitrification in nitrate-rich aquatic ecosystems can be inferred from these linear relationships. Our method allowed the determination of field-scale *in situ* N₂ fluxes from nitrate-rich aquatic ecosystems both with and without overlaying water. The perturbation-free *in situ* N₂ fluxes observed by the new method were almost one order of magnitude higher than those by the sediment core method. The ability of aquatic ecosystems to remove Nr may previously have been severely underestimated.

© 2016 Elsevier Ltd. All rights reserved.

1. Introduction

Globally, the creation of reactive nitrogen (Nr) via anthropogenic activities has accelerated from 15.3 Tg N yr⁻¹ in 1910 to 187 Tg N yr⁻¹ in 2005, and further to 210 Tg N yr⁻¹ in 2010 (Galloway et al., 2008; Cui et al., 2013; Fowler et al., 2013). Excess Nr threatens the quality of air, soil and water (Sutton et al., 2011). Some Nr species, especially nitrate, will be converted back into inert dinitrogen (N₂) through denitrification (Seitzinger, 2008). However, there is a large uncertainty associated with estimating the amount of Nr denitrified back into inert N₂ since robust methods are still not readily available for perturbation-free *in situ* N₂ fluxes

determinations. This is especially true for nitrate-rich aquatic ecosystems (Seitzinger, 2008). The available methods, e.g., the ¹⁵N enrichment method, acetylene inhibition technique and the sediment core method, perturb the ecosystems under study and consequently cause large uncertainties in N₂ fluxes (Devol, 1991; Piña-Ochoa and Álvarez-Cobelas, 2006; Schlesinger, 2009; Duncan et al., 2013; Li et al., 2013). An integrated, whole-ecosystem approach based on membrane inlet mass spectrometry has been previously developed to quantify *in situ* N₂ emission from rivers (Laursen and Seitzinger, 2002). This is a powerful method for perturbation-free N₂ flux determination but applicable only with overlaying water because the N₂ fluxes are calculated using the measurements of dissolved N₂ concentrations in the overlaying waters (Laursen and Seitzinger, 2005). Wetland sediments are periodically exposed to atmosphere due to the variation in water

* Corresponding author.

E-mail addresses: meimei841114@163.com, cshu@sjziam.ac.cn (C. Hu).

levels, during which significant N₂ emissions into atmosphere may occur (Kern et al., 1996). Additionally, the aquatic-terrestrial transition zones (riparian buffer zones) have been reported to remove large amounts of N_r from wetland ecosystems (Hefting et al., 2003). There remains a need to develop new methods to determine *in situ* N₂ fluxes from sediments both with and without overlaying water (Davidson and Seitzinger, 2006; Groffman et al., 2006). Development of such methods will help to comprehensively evaluate the N₂ fluxes from wetland ecosystems.

Both nitrous oxide (N₂O) and N₂ are simultaneously emitted from nitrate-rich sediments following microbially-mediated denitrification. Denitrifiers preferentially reduce N₂O molecules that contain the lighter ¹⁴N stable isotope, which leads to increasing ¹⁵N enrichment of the remaining N₂O (Ostrom et al., 2007; Vieten et al., 2007), a phenomenon known as isotopic fractionation (Ostrom et al., 2007). Theoretically, the larger the reduction of N₂O by microorganisms, the higher the δ¹⁵N-N₂O signature of N₂O emitted into the atmosphere. In this study, we firstly verified two assumptions, i.e., i) the dynamics in the δ¹⁵N-N₂O signature of the emitted N₂O from nitrate-rich sediments are predominantly controlled by reduction; and ii) the δ¹⁵N-N₂O signature of N₂O emitted into the atmosphere is related to the N₂O/(N₂+N₂O) emission ratios. After verifying these assumptions, we hypothesized that the perturbation-free N₂ fluxes from a nitrate-rich river sediment could be inferred from the relationships between the δ¹⁵N-N₂O signatures and the N₂O/(N₂+N₂O) emission ratios. We assumed equilibrium between the gas and solute phases for both N₂O and N₂.

2. Materials and methods

2.1. Sediment sampling

Intact sediment cores were sampled from the Hutuo River in Hebei Province, China, using a hollow PVC cylinder (220 mm in inner diameter, 160 mm in length). In order to comprehensively test the proposed assumptions and hypothesis, we collected four sediments (no. 1, 2, 3 and 4) with different clay contents along the Hutuo River. The locations of the sampling sites are shown in Fig. 1. The sampling times for each location are shown in Table 1. For each location, three intact sediment cores were collected for each sampling time. At the same time, four additional small sediment cores (3.2 cm in diameter, 140 mm in depth) were collected to test the proposed assumptions. The collected soil cores were transported to the laboratory within 2 h and stored at 4 °C. All of the analyses were finished within one week.

2.2. Verification of assumption i)

Assumption i) was verified by the acetylene (C₂H₂) addition experiment. The procedure was as follows: equivalents of 10 g (oven dry weight) of either sediment no. 1 or 2 were added into 24 serum flasks (120 ml). Then 20 ml of 1 mM glucose solution and a magnetic stirring bar were added into each flask. The flasks were sealed with an air-tight butyl rubber septa and aluminum cap, and brought to vacuum and filled with an artificial N₂-free atmosphere (99.999% helium) five times until the N₂ concentration was below 30 ppmv. A preliminary experiment indicated that repeatedly exposing the soil to a vacuum (0.1 k Pa) had no statistically significant effects on soil respiration, suggesting that the microbial activity was not negatively affected (Qin et al., 2012). For each flask, 10 ml of C₂H₂ was injected into the flask with an air-tight syringe after removing an equal amount of headspace gas from the flask. The final C₂H₂ concentration in the headspace of the flask was 10% (v/v). Finally, the flasks were incubated in a thermostatically

controlled water bath at 125 rev min⁻¹ and 25 °C. Non-C₂H₂ control samples were identically treated except for the C₂H₂ addition. Four flasks were used to monitor N₂O and N₂ emissions. The other 20 flasks were used to monitor the δ¹⁵N-N₂O signatures. The dynamics of N₂O and N₂ concentrations in the headspace were monitored using a robotized sampling and analyzing system, similar to that described by Molstad et al. (2007). This robotized system had the advantage of minimizing N₂ leaks during sampling. Briefly, the system consisted of a gas chromatograph (GC, Agilent 7890) coupled to a peristaltic pump, an auto-sampler and a thermostatically controlled water bath. The δ¹⁵N-N₂O signatures in the headspace were determined by an isotope ratio mass spectrometer. Before δ¹⁵N-N₂O signature measuring, the gas samples were washed with 0.1% potassium permanganate solution to remove C₂H₂ to avoid the C₂H₂ interference with the mass spectrometer. Preliminary experiments showed that washing the gas samples by 0.1% potassium permanganate solution slightly decreased the N₂O concentration but did not significantly affected the δ¹⁵N-N₂O signatures (data not shown).

2.3. Verification of assumption ii)

Assumption ii) was verified by the glucose/acetate addition experiments. We used these two carbon sources to test whether different carbon sources yielded similar functions between the logarithmically transformed N₂O/(N₂+N₂O) emission ratios and the δ¹⁵N-N₂O signatures.

2.3.1. Glucose addition experiment

Glucose was added into the sediment to obtain a range of N₂O/(N₂+N₂O) emission ratios (Raut et al., 2012). Again the equivalents of 10 g sediment (oven dry weight) were added into 120 ml serum flasks. Then 20 ml of solution (1 mM glucose) and a magnetic stirring bar were added into each flask. The flasks were sealed with air-tight butyl rubber septa and aluminum caps, and brought to vacuum (0.1 k Pa) and filled with an artificial N₂-free gas (79% He and 21% O₂) five times. The flasks were incubated in a thermostatically controlled water bath at 25 °C. Before incubation, the slurries were homogenized by magnetic stirring at 125 rev min⁻¹ for 30 s. The N₂O and N₂ concentrations and δ¹⁵N-N₂O values in the headspace were measured as noted in the C₂H₂ addition experiment. The functions between the logarithmically transformed N₂O/(N₂+N₂O) emission ratios and the δ¹⁵N-N₂O signatures were fitted using the Sigma-Plot software, version 12.5 (Systat Soft-ware, San Jose, CA, USA).

2.3.2. Sodium acetate addition experiment

A sodium acetate addition experiment was performed identical to the glucose addition experiment, except that 1 mM glucose was replaced by 1 mM sodium acetate.

2.4. Hypothesis testing

The hypothesis was tested by the sediment core method. In this method, the N₂ surrounding and within the sediment cores was substituted by an artificial N₂-free gas (79% He and 21% O₂) to determine the trace N₂ emissions. A simple cylinder-in-cylinder setup was developed to lower inward N₂ leakage from the atmosphere and consequently to directly determine N₂ emissions from the sediment cores. This setup consisted of an inner and an outer cylinder. The interlayer between the two cylinders acts as a low-N₂ buffer against N₂ leakage from atmosphere. The details of the construction and the operation of the cylinder-in-cylinder setup are described in the Supplemental Information. The procedure was as follows: fresh sediment cores were put into the inner cylinder

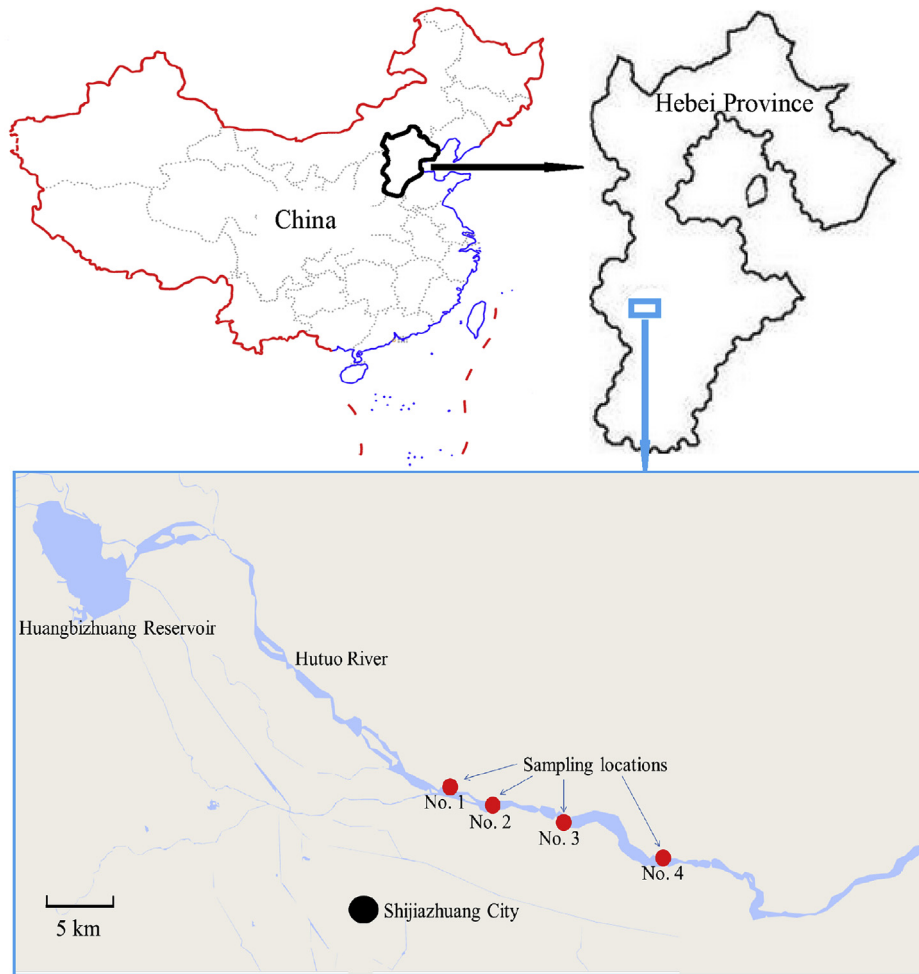


Fig. 1. Legend for the locations of the sampling sites.

(diameter 220 mm, height 160 mm). For sediments collected in 2013, 20 mm overlaying river water was retained over the sediment cores; for sediment cores collected in 2016, no overlaying water was retained over the sediment cores. The inner cylinder was sealed with an air-tight butyl rubber septum and a stainless-steel cap, brought to vacuum and filled with an artificial N_2 -free atmosphere (79% helium and 21% oxygen) five times until the N_2 concentration in the headspace of the inner cylinder was below 300 ppmv. Then the inner cylinder was placed into the outer cylinder ($\Phi 260$ mm, height 180 mm). The outer cylinder was sealed with a stainless-steel cap and an air-tight butyl rubber septum. The interlayer between the two cylinders was brought to vacuum and replenished with N_2 -free gas (79% helium and 21% oxygen) five times until the N_2 concentration was below 300 ppmv. The dynamics of the N_2O and N_2 concentrations and $\delta^{15}N-N_2O$ were monitored identically to the C_2H_2 addition experiment. The measured N_2 fluxes were compared with those inferred from the functions in Table 1.

2.5. Perturbation-free measurement of N_2 fluxes from *in situ* sediments

The perturbation-free *in situ* N_2 fluxes from denitrification were determined by the static chamber method (Horvath et al., 2006). The chamber size (length \times width \times height) was 60 cm \times 20 cm \times 40 cm. Each chamber was equipped with a

manual fan to ensure complete gas mixing. Polypropylene chamber bases were gently inserted into the sediment to a depth of approximately 1 cm. The headspaces of the chambers were gently filled with overlying water and flushed with an N_2O -free artificial atmosphere (79% N_2 , 21% O_2) to exclude the initial N_2O in the headspace. Gas samples were collected from the chambers with 60 ml polypropylene syringes equipped with three-way stopcocks at 10, 20, 40 and 60 min after the chambers were installed. The N_2O concentrations and $\delta^{15}N-N_2O$ signatures in the gas samples were analyzed by GC and isotope mass spectrometry, respectively, within 24 h of collection. The N_2O flux was calculated based on the rate of change in N_2O concentration within the chamber, which was estimated as the slope of linear regression between concentration and time. The $N_2O/(N_2+N_2O)$ emission ratios were calculated based on the $\delta^{15}N-N_2O$ values measured *in situ* and the regressions in Table 1. The perturbation-free *in situ* N_2 fluxes were inferred based on the $N_2O/(N_2+N_2O)$ emission ratios and the N_2O fluxes measured by the static chamber method.

3. Results and discussion

3.1. Verification of assumption i): the dynamics in the $\delta^{15}N-N_2O$ signature of the emitted N_2O from nitrate-rich river sediments are predominantly controlled by reduction

Our result showed that C_2H_2 almost completely stopped

Table 1

Measured and inferred N_2 fluxes from sediments. The N_2 fluxes are presented as mean \pm SD ($n = 3$). Different sediment numbers (1, 2, 3 and 4) indicate the sampling locations as shown in Fig. 1.

Sediments		Functions between $\delta^{15}N-N_2O$ (x) and the ratio of logarithmically transformed $N_2O/(N_2O + N_2)$ emission ratios (y)	N_2 fluxes ($\mu mol m^{-2} h^{-1}$)	
No.	Collection date		Determined by the sediment core method in the lab	<i>In situ</i> determined by the static chamber method
1	March 2013	$y = -0.16 \times -6.36$ $R^2 = 0.98$	1.4 ± 1.1 a	12.1 ± 9.5 b
	April 2013	$y = -0.19 \times -5.59$ $R^2 = 0.95$	3.5 ± 2.7 a	28.9 ± 27.8 b
	May 2013	$y = -0.17 \times -5.94$ $R^2 = 0.97$	20.4 ± 7.1 a	85.5 ± 25.4 b
	September 2016	$y = -0.16 \times -7.03$ $R^2 = 0.95$	13.56 ± 5.4 a	26.84 ± 13.2 a
2	October 2013	$y = -0.08 \times -4.14$ $R^2 = 0.89$	2.6 ± 3.1 a	10.8 ± 9.3 a
	November 2013	$y = -0.08 \times -3.31$ $R^2 = 0.98$	2.0 ± 1.5 a	12.9 ± 8.1 b
	September 2016	$y = -0.06 \times -4.07$ $R^2 = 0.85$	3.56 ± 2.1 a	16.47 ± 11.04 b
3	May 2013	$y = -0.26 \times -9.41$ $R^2 = 0.98$	47.5 ± 15.5 a	128.6 ± 49.5 b
4	October 2013	$y = -0.02 \times -4.44$ $R^2 = 0.78$	0.8 ± 0.1 a	2.6 ± 1.5 b
	November 2013	$y = -0.01 \times -4.21$ $R^2 = 0.32$	0.4 ± 0.2 a	0.3 ± 0.6 a
	December 2013	$y = -0.05 \times -3.32$ $R^2 = 0.77$	0.5 ± 0.2 a	3.8 ± 2.4 b

Different letters in the same rows indicate significant difference at $p < 0.05$.

microbial N_2O reduction (Fig. 2). Apart from inhibiting N_2O reduction, C_2H_2 can also inhibit nitrification (Walter et al., 1979). In the present study, the dissolved oxygen contents in the pore water of the sediments were low (in most layers below $2 mg L^{-1}$, Fig. 3), indicating that nitrification rates would not be high. Additionally, the nitrate concentrations in the overlying water and the pore water of the sediments were high (above $20 mg NO_3^- L^{-1}$, Fig. 3), indicating that the possible inhibition of C_2H_2 on nitrification did not significantly affect the nitrate supply in this study. C_2H_2 has been reported to be decomposed by microorganisms after 7-d incubation (Terry and Duxbury, 1985). In this study, the sediments were incubated for only 8 and 15 h. Consequently, significant decomposition of C_2H_2 was unlikely in this relatively short incubation and the remaining C_2H_2 was sufficient to inhibit N_2O reduction, as was proven by the continually increasing N_2O concentration (Fig. 2).

The $\delta^{15}N-N_2O$ values in the beginning of the incubation ranged from -22‰ to -16‰ (Fig. 2). The major source partitions for N_2O are ammonia oxidation, nitrifier denitrification and denitrification (Decock and Six, 2013). Each of these source partitions has a specific range of $\delta^{15}N-N_2O$ values (Decock and Six, 2013). The $\delta^{15}N-N_2O$ values in this study were mostly consistent with those produced through denitrification (Decock and Six, 2013), indicating that denitrification was the dominant source for N_2O production. The dissolved oxygen contents decreased dramatically with increasing sediment depth (Fig. 3), which also indicated that denitrification dominated N_2O emission in this study. C_2H_2 addition in this study did not significantly alter the $\delta^{15}N-N_2O$ values at the beginning of the incubation (Fig. 2). This result indicated that the C_2H_2 addition had limited effects on N_2O source partitions in the present study. The $\delta^{15}N-N_2O$ signatures increased significantly in the absence of C_2H_2 due to N_2O reduction, but stabilized when it was present (Fig. 2). The latter was probably due to the fact that nitrate was not limiting in this system ($20\text{--}40 mg L^{-1}$) (Fig. 3). The above results indicated that N_2O reduction accounted for the dynamics in $\delta^{15}N-N_2O$ for these river sediments. Consequently, assumption i) was verified.

3.2. Verification of assumption ii): the $\delta^{15}N-N_2O$ signature of N_2O emitted into the atmosphere is related to the $N_2O/(N_2+N_2O)$ emission ratios

Dissolved carbon concentration has been reported to significantly affect $N_2O/(N_2+N_2O)$ emission ratios (Raut et al., 2012). In this study, we added glucose/sodium acetate into sediments to mediate the $N_2O/(N_2+N_2O)$ emission ratios and expected to develop a range of $N_2O/(N_2+N_2O)$ emission ratios with the depletion of glucose/sodium acetate by microbial respiration. The logarithmically transformed $N_2O/(N_2+N_2O)$ emission ratios showed significantly negative linear correlations with $\delta^{15}N-N_2O$ values in this study (Fig. 4). The sodium acetate addition experiment yielded similar functions between the $N_2O/(N_2+N_2O)$ emission ratios and the $\delta^{15}N-N_2O$ values (Fig. 5), indicating that carbon sources had little effects on these functions.

Clay content is one of the key factors affecting N_2O transportation and consequently affecting N_2O residence time in sediments (Baulch et al., 2011). In this study, we collected four sediments with distinct clay contents ($7\text{--}34\%$, Fig. 3) to test whether assumption ii) was valid for different sediments. The results showed that the logarithmically transformed $N_2O/(N_2+N_2O)$ emission ratios were linearly correlated with the $\delta^{15}N-N_2O$ signature of N_2O in all of the four sediments. Consequently, assumption ii) was also verified. The slopes of the linear functions were similar for the same sediment when collected at different times, but differed among sediments (Fig. 4). The variation in the slopes among sediments was probably related to differences in the microbial community structure of denitrifiers, since different denitrifiers may emit N_2O with different isotopic signatures (Santoro et al., 2011). Sampling times and locations significantly affected the convergence (R^2 values) of the functions between the $\delta^{15}N-N_2O$ signatures and logarithmically transformed $N_2O/(N_2+N_2O)$ emission ratios. Low R^2 values were observed in sediments with low N_2 fluxes (Table 1). A possible reason was that the dissolved N_2O in the water phase, which was not considered in this study, could have contributed significantly to the total N_2O emission from the

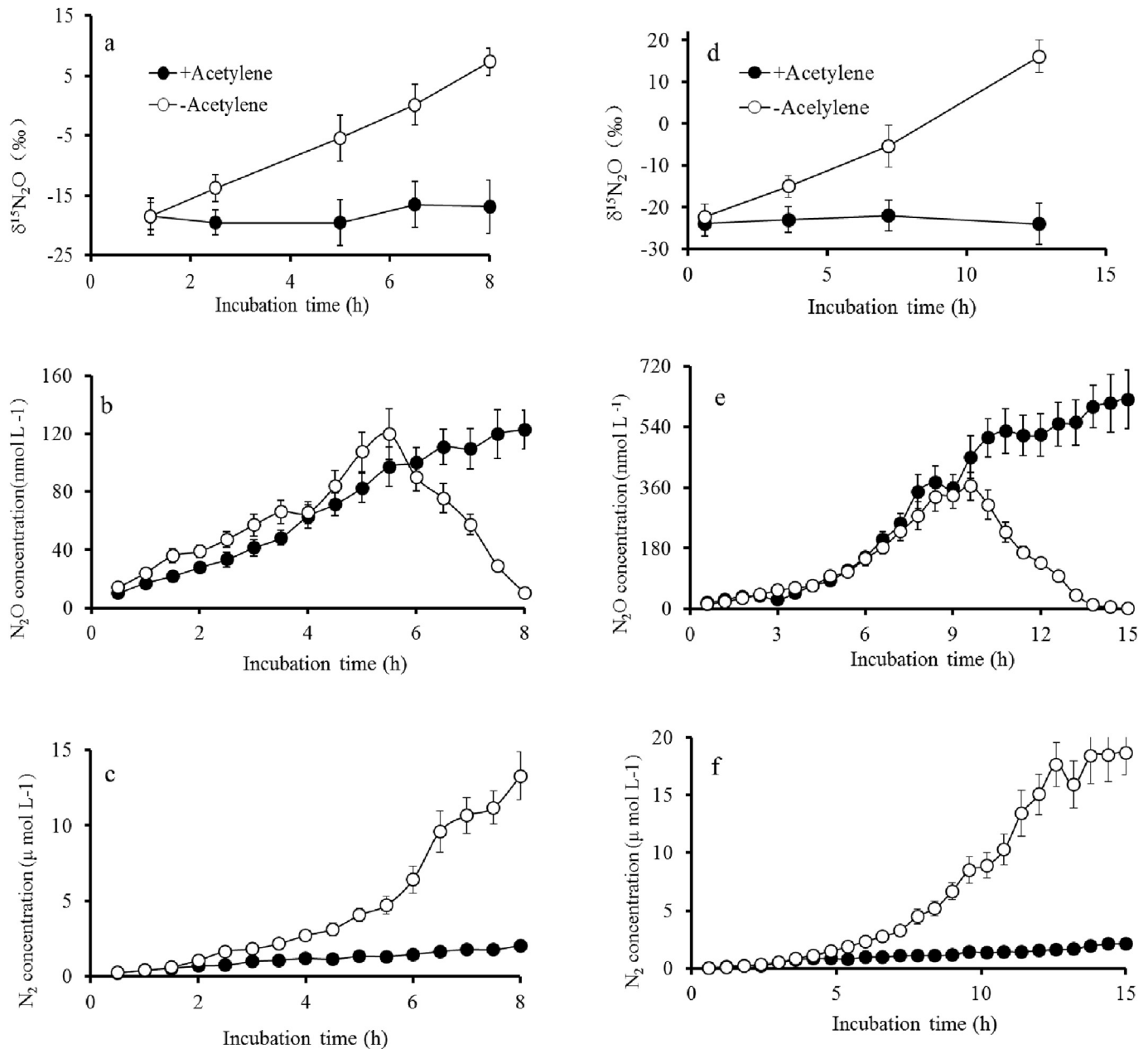


Fig. 2. Acetylene addition effects on cumulative N_2O and N_2 fluxes and the $\delta^{15}N-N_2O$ signature of the cumulative N_2O emissions in sediments no. 1 (a, b, c) and 2 (d, e, f). Data points are means \pm SD ($n = 4$).

sediments with low denitrification rate. These results indicated that the isotopic method proposed in this study is more reliable in sediments with high denitrification rates.

3.3. Verification of the hypothesis: the *in situ* N_2 fluxes from a nitrate-rich aquatic system could be inferred from the relationships between $\delta^{15}N-N_2O$ and the $N_2O/(N_2+N_2O)$ emission ratios

To test the hypothesis, we developed a novel cylinder-in-cylinder setup to directly measure the N_2 fluxes from river sediments in the laboratory (Fig. S1). The interlayer between the two cylinders acted as a gas buffer against atmospheric N_2 leakage (Fig. S1). Tightness tests showed that this setup dramatically lowered the N_2 leakage (Fig. S3). On one hand, we directly measured the N_2 and N_2O fluxes and the $\delta^{15}N-N_2O$ signatures using the

cylinder-in-cylinder setup. On the other hand, we calculated the N_2 fluxes derived from the linear relationships between the $N_2O/(N_2+N_2O)$ emission ratios and the $\delta^{15}N-N_2O$ signatures in Table 1, and compared these with the directly measured N_2 fluxes, to test the hypothesis. The results showed that, for the sediments with overlying water, the inferred N_2 fluxes tended to be slightly lower than the directly measured N_2 fluxes, especially for the sediments with higher N_2 fluxes (Fig. 6), while for the sediments without overlying water, the inferred and the directly measured N_2 fluxes were comparable (Fig. 6). The difference was probably due to the dissolved N_2O in the water phase, which was not measured in this study. But taken as whole, the calculated and measured N_2 fluxes were comparable both with and without overlying water ($R^2 > 0.8$, Fig. 6), hence the N_2 fluxes, at least their orders of magnitude, can be inferred from the measurements of N_2O emissions and their

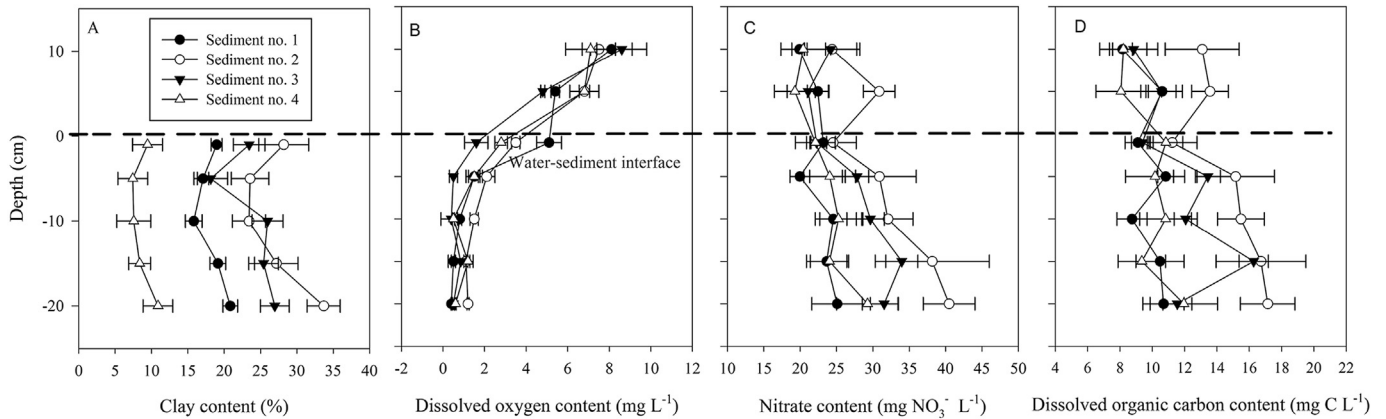


Fig. 3. Clay (A), dissolved oxygen (B), nitrate (C) and dissolved organic carbon (D) concentrations in overlaying water and sediments. For sediments no. 1, 2, 3 and 4, the data represents the samples collected in March 2013, October 2013, May 2013 and October 2013, respectively.

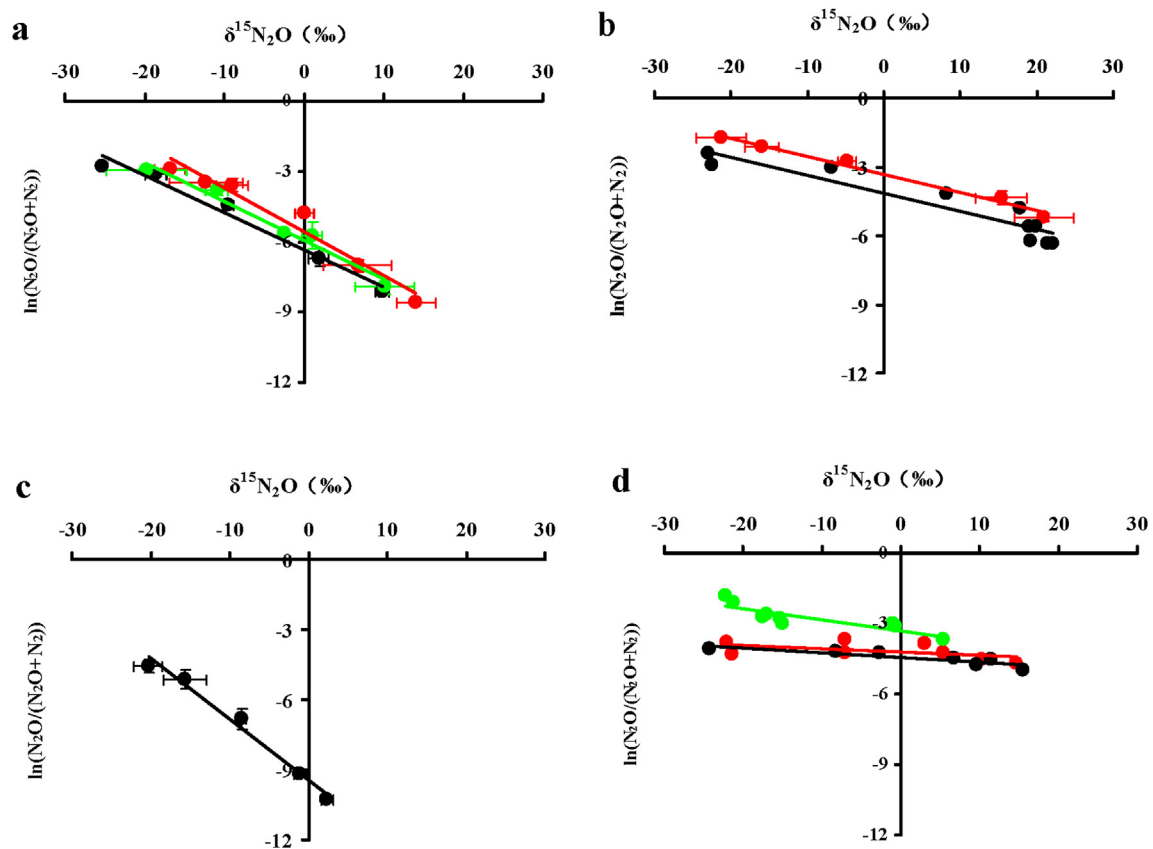


Fig. 4. Logarithmically transformed $N_2O/(N_2+N_2O)$ emission ratios as functions of $\delta^{15}N-N_2O$ in sediments no. 1 (a), 2 (b), 3 (c) and 4 (d). Sediment no. 1 was collected in March 2013 (black symbol), in April 2013 (red symbol) and in May 2013 (green symbol). Sediment no. 2 was collected in October (black symbol) and November (red symbol) 2013. Sediment no. 3 was collected in May 2013 (black symbol). Sediment no. 4 was collected in October (black symbol), November (red symbol) and December (green symbol) 2013. (For interpretation of the references to colour in this figure legend, the reader is referred to the web version of this article.)

isotopic signatures. Consequently, the hypothesis was verified.

3.4. Perturbation-free measurement of N_2 fluxes from *in situ* sediments

We then measured *in-situ* the N_2O fluxes and the $\delta^{15}N-N_2O$ signatures using a static chamber method, and inferred the N_2 fluxes from the linear relationships between the logarithmically transformed $N_2O/(N_2+N_2O)$ emission ratios and the $\delta^{15}N-N_2O$

signatures in Table 1. We compared our perturbation-free *in situ* method with a traditional method (the sediment core method). The results showed that the N_2 fluxes measured by the sediment core method ranged from 0.4 to 47.5 $\mu\text{mol m}^{-2} \text{h}^{-1}$ (Table 1), depending on sampling sites and seasons. These N_2 fluxes fall within the range of N_2 fluxes (0–344 $\mu\text{mol m}^{-2} \text{h}^{-1}$) previously reported for estuarine, river and coastal sediments where the N_2 fluxes were measured by the acetylene inhibition technique, the ^{15}N enrichment method or the sediment core method (Binnerup et al., 1992;

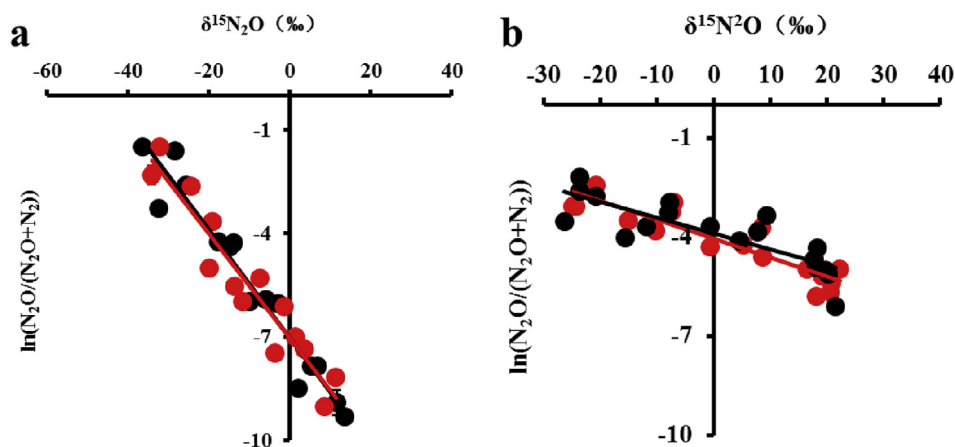


Fig. 5. Effects of carbon sources on the functions between the $N_2O/(N_2+N_2O)$ emission ratios and $\delta^{15}N-N_2O$ in sediments no. 1 (a) and 2 (b). Sediments were amended with 1 mM glucose (red circles) and sodium acetate (black circles) solution and incubated under anaerobic conditions. The sediments samples were collected on September 18, 2016. (For interpretation of the references to colour in this figure legend, the reader is referred to the web version of this article.)

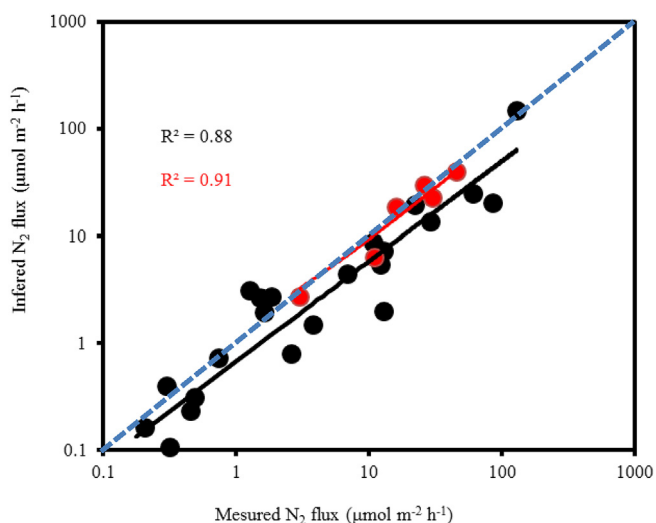


Fig. 6. Relationship between the measured N_2 fluxes and the inferred N_2 fluxes from the equations in Table 1 for sediments with overlying water (black circles) and without overlying water (red circles). The blue dashed line indicates 1:1 correlation line. (For interpretation of the references to colour in this figure legend, the reader is referred to the web version of this article.)

Lamontagne and Valiela, 1995; Fulweiler and Nixon, 2011). The perturbation-free *in situ* N_2 fluxes measured in this study ranged from 0.3 to 128.6 $\mu\text{mol m}^{-2} \text{h}^{-1}$ and were almost one order of magnitude larger than those measured by the sediment core method (Table 1). The difference probably resulted from the blocking of horizontal and vertical nitrate recharge by the sediment core method.

These results indicate that the sediment core method runs the risk of underestimating N_2 fluxes from denitrification for aquatic sediments. The method described here provides an approach to overcome this underestimation since it avoids the artificial disturbance on sediment ecosystems and consequently yields N_2 fluxes similar to those under natural conditions. Additionally, this method is applicable to sediments both with and without overlying water. This means that the method has the potential to contribute to more comprehensive evaluation of N_2 fluxes from aquatic ecosystems by taking into account the N_2 fluxes from riparian buffer zones and from sediments without overlying water during low water periods.

4. Conclusion

Our results show that strong relationships exist between the $\delta^{15}N-N_2O$ signatures and the logarithmically transformed $N_2O/(N_2+N_2O)$ emission ratios. The perturbation-free *in situ* N_2 fluxes from denitrification in nitrate-rich sediments can be inferred from the measurements of N_2O emissions and the $\delta^{15}N-N_2O$ signatures.

The method described here has some limitations. First of all, assumption i) is not valid for nitrate-limited sediments because the isotopic fractionations in both N_2O and nitrate reductions contribute significantly to the dynamics in the $\delta^{15}N-N_2O$ signature. Consequently, this method is applicable only to nitrate-rich aquatic ecosystems. Secondly, the method has relatively greater bias in sediments with low N_2 fluxes. Thirdly, the linear functions between the $\delta^{15}N-N_2O$ signatures and the logarithmically transformed $N_2O/(N_2+N_2O)$ emission ratios changed significantly among different sediments. This means that a site-specific function is needed to be developed before using this method in a new site. Further studies are needed to investigate the dependences of the functions on sediment properties to further facilitate the application of this method.

Even with the above limitations, the method described here has the advantage of being applicable to sediments both with and without overlying water and creates minimal artificial disturbance on the investigated ecosystem. It has the potential to complement other methods, to quantify the *in situ* aquatic N_2 fluxes more comprehensively and precisely.

Acknowledgments

We are thankful to Lars Molstad, UMB Nitrogen group, Norwegian University of Life Sciences for providing software and constructing the robotized incubation system for analyzing gas kinetics. This work was supported by the National Natural Science Foundation of China (No. 41301323, 312780554 and 41530859).

Appendix A. Supplementary data

Supplementary data related to this article can be found at <http://dx.doi.org/10.1016/j.watres.2016.11.035>.

References

Baulch, H.M., Dillon, P.J., Maranger, R., Schiff, S.L., 2011. Diffusive and ebullitive

- transport of methane and nitrous oxide from streams: are bubble-mediated fluxes important? *J. Geophys. Res.* 116 (G4), G04028.
- Binnerup, S.J., Jensen, K., Revsbech, N.P., Jensen, M.H., Sørensen, J., 1992. Denitrification, dissimilatory reduction of nitrate to ammonium, and nitrification in a bioturbated estuarine sediment as measured with ^{15}N and microsensor techniques. *Appl. Environ. Microbiol.* 58 (1), 303–313.
- Cui, S., Shi, Y., Groffman, P.M., Schlesinger, W.H., Zhu, Y.G., 2013. Centennial-scale analysis of the creation and fate of reactive nitrogen in China (1910–2010). *Proc. Natl. Acad. Sci. U. S. A.* 110 (6), 2052–2057.
- Davidson, E.A., Seitzinger, S., 2006. The enigma of progress in denitrification research. *Ecol. Appl.* 16 (6), 2057–2063.
- Decock, C., Six, J., 2013. How reliable is the intramolecular distribution of ^{15}N in N_2O to source partition N_2O emitted from soil? *Soil Biol. Biochem.* 65 (11), 114–127.
- Devol, A.H., 1991. Direct measurement of nitrogen gas fluxes from continental shelf sediments. *Nature* 349 (6307), 319–321.
- Duncan, J.M., Groffman, P.M., Band, L.E., 2013. Towards closing the watershed nitrogen budget: spatial and temporal scaling of denitrification. *J. Geophys. Res.* 118 (3), 1105–1119.
- Fowler, D., Coyle, M., Skiba, U., Sutton, M.A., Cape, J.N., Reis, S., Sheppard, L.J., Jenkins, A., Grizzetti, B., Galloway, J.N., Vitousek, P., Leach, A., Bouwman, A.F., Butterbach-Bahl, K., Dentener, F., Stevenson, D., Amann, M., Voss, M., 2013. The global nitrogen cycle in the twenty-first century. *Philos. Trans. R. Soc. B* 368 (1621), 1621.
- Fulweiler, R.W., Nixon, S.W., 2011. Net sediment N_2 fluxes in a southern New England estuary: variations in space and time. *Biogeochemistry* 111 (1–3), 111–124.
- Galloway, J.N., Townsend, A.R., Erisman, J.W., Bekunda, M., Cai, Z., Freney, J.R., Martinelli, L.A., Seitzinger, S.P., Sutton, M.A., 2008. Transformation of the nitrogen cycle: recent trends, questions, and potential solutions. *Science* 320 (5878), 889–892.
- Groffman, P.M., Altabet, M.A., Böhlke, J.K., Butterbach-Bahl, K., David, M.B., Firestone, M.K., Giblin, A.E., Kana, T.M., Nielsen, L.P., Voytek, M.A., 2006. Methods for measuring denitrification: diverse approaches to a difficult problem. *Ecol. Appl.* 16 (6), 2091–2122.
- Hefting, M.M., Bobbink, R., de Caluwe, H., 2003. Nitrous oxide emission and denitrification in chronically nitrate-loaded riparian buffer zones. *J. Environ. Qual.* 32 (4), 1194–1203.
- Horvath, L., Fuhrer, E., Lajtha, K., 2006. Nitric oxide and nitrous oxide emission from Hungarian forest soils; linked with atmospheric N-deposition. *Atmos. Environ.* 40 (40), 7786–7795.
- Kern, J., Darwich, A., Furch, K., Junk, W.J., 1996. Seasonal denitrification in flooded and exposed sediments from the Amazon floodplain at Lago Camaleão. *Microb. Ecol.* 32 (1), 47–57.
- Lamontagne, M.G., Valiela, I., 1995. Denitrification measured by a direct N_2 flux method in sediments of Waquoit Bay, MA. *Biogeochemistry* 31 (2), 63–83.
- Laursen, A., Seitzinger, S., 2002. Measurement of denitrification in rivers: an integrated, whole reach approach. *Hydrobiologia* 485 (1–3), 67–81.
- Laursen, A., Seitzinger, S., 2005. Limitations to measuring riverine denitrification at the whole reach scale: effects of channel geometry, wind velocity, sampling interval, and temperature inputs of N_2 -enriched groundwater. *Hydrobiologia* 545 (1), 225–236.
- Li, X., Xia, Y., Li, Y., Kana, T., Kimura, S., Saito, M., Yan, X., 2013. Sediment denitrification in waterways in a rice-paddy-dominated watershed in eastern China. *J. Soils Sediments* 13 (4), 783–792.
- Molstad, L., Dorsch, P., Bakken, L.R., 2007. Robotized incubation system for monitoring gases (O_2 , NO , N_2O and N_2) in denitrifying cultures. *J. Microbiol. Methods* 71 (3), 202–211.
- Ostrom, N.E., Pitt, A., Sutka, R., Ostrom, P.H., Grandy, A.S., Huizinga, K.M., Robertson, G.P., 2007. Isotopologue effects during N_2O reduction in soils and in pure cultures of denitrifiers. *J. Geophys. Res. Biogeosci.* 112 (G2), G02005.
- Piña-Ochoa, E., Álvarez-Cobelas, M., 2006. Denitrification in aquatic environments: a cross-system analysis. *Biogeochemistry* 81 (1), 111–130.
- Qin, S.P., Hu, C.S., Oenema, O., 2012. Quantifying the underestimation of soil denitrification potential as determined by the acetylene inhibition method. *Soil Biol. Biochem.* 47 (3–4), 14–17.
- Raut, N., Dorsch, P., Sitaula, B.K., Bakken, L.R., 2012. Soil acidification by intensified crop production in South Asia results in higher $\text{N}_2\text{O}/(\text{N}_2+\text{N}_2\text{O})$ product ratios of denitrification. *Soil Biol. Biochem.* 55 (12), 104–112.
- Santoro, A.E., Buchwald, C., McIlvin, M.R., Casciotti, K.L., 2011. Isotopic signature of N_2O produced by marine ammonia-oxidizing archaea. *Science* 333 (6047), 1282–1285.
- Schlesinger, W.H., 2009. On the fate of anthropogenic nitrogen. *Proc. Natl. Acad. Sci. U. S. A.* 106 (1), 203–208.
- Seitzinger, S., 2008. Nitrogen cycle: out of reach. *Nature* 452 (7184), 162–163.
- Sutton, M.A., Oenema, O., Erisman, J.W., Leip, A., Grinsven, H., 2011. Too much of a good thing. *Nature* 472 (7342), 159–161.
- Terry, R.E., Duxbury, J.M., 1985. Acetylene decomposition in soils. *Soil Sci. Soc. Am. J.* 49 (1), 90–94.
- Vieten, B., Blunier, T., Neftel, A., Alewell, C., Conen, F., 2007. Fractionation factors for stable isotopes of N and O during N_2O reduction in soil depend on reaction rate constant. *Rapid Commun. Mass Spectrom.* 21 (6), 846–850.
- Walter, H.M., Keeney, D.R., Fillery, I.R., 1979. Inhibition of nitrification by Acetylene. *Soil Sci. Soc. Am. J.* 43 (1), 195–196.